Bull Math Biol (2013) 75:2059–2078
DOI 10.1007/s11538-013-9880-z

Society for Mathematical Biology

ORIGINAL ARTICLE

Complex Dynamics in an Eco-epidemiological Model

Andrew M. Bate · Frank M. Hilker

Received: 23 November 2012 / Accepted: 16 July 2013 / Published online: 18 September 2013

Abstract The presence of infectious diseases can dramatically change the dynamics of ecological systems. By studying an SI-type disease in the predator population of a Rosenzweig–MacArthur model, we find a wealth of complex dynamics that do not exist in the absence of the disease. Numerical solutions indicate the existence of saddle–node and subcritical Hopf bifurcations, turning points and branching in periodic solutions, and a period-doubling cascade into chaos. This means that there are regions of bistability, in which the disease can have both a stabilising and destabilising effect. We also find tristability, which involves an endemic torus (or limit cycle), an endemic equilibrium and a disease-free limit cycle. The endemic torus seems to disappear via a homoclinic orbit. Notably, some of these dynamics occur when the basic reproduction number is less than one, and endemic situations would not be expected at all. The multistable regimes render the eco-epidemic system very sensitive to perturbations and facilitate a number of regime shifts, some of which we find to be irreversible.

Keywords Eco-epidemiology · Period-doubling · Chaos · Bistability · Tristability

1 Introduction

Complex dynamics like bistability, quasiperiodicity and chaos have been found in isolation in many ecological, epidemiological and eco-epidemiological models. Such complex dynamics mean that small changes to parameters or initial conditions can have large effects on the biological system in the long term. In this paper, two relatively simple eco-epidemiological models are investigated; both models are of

A.M. Bate (✉) · F.M. Hilker
Centre for Mathematical Biology, Department of Mathematical Sciences, University of Bath, Bath BA2 7AY, UK
e-mail: A.M.Bate@bath.ac.uk

Rosenzweig–MacArthur predator–prey type with an SI disease in the predator with different forces of infection. Within these models, a multitude of different forms of bistability are found, as well as a torus bifurcation, a period-doubling cascade into chaos and even an example of tristability. This diversity of complex dynamics has rarely been seen in one investigation.

Some of these complex dynamics have been discovered in ecology. For example, May (1974) demonstrated that simple discrete-time single-species models can exhibit chaos. However, in continuous-time models, three species are needed to produce more complex dynamics than just equilibria and limit cycles (Seydel 1988). Gilpin (1979) found the first example of chaos in a continuous-time ecological model while investigating a one-predator–two-prey model, whereas Hastings and Powell (1991) found chaos in a three-species food chain. Bistability is something that has long been established in ecology. One famous example of bistability is the two-species Lotka–Volterra competition model. Likewise, in epidemiology, there exist backward bifurcations with saddle–node bifurcations in several models creating bistability between endemic and disease-free equilibria (van den Driessche and Watmough 2002).

Within the field of eco-epidemiology, there are a few studies that demonstrate some of these complex dynamics. Hilker and Malchow (2006) found a "strange periodic" attractor, which seems to be a toric transient that lasts for a substantial time period. Sieber and Hilker (2011) go further than Hilker and Malchow (2006) by demonstrating that chaos, bistability and attractor crises can also occur. The first eco-epidemiological paper to show chaos is Upadhyay et al. (2008), using an existing model (Chattopadhyay and Bairagi 2001), presumably via a cascade of period-doubling bifurcations. Stiefs et al. (2009) demonstrate that quasiperiodicity and chaos exist in a generalised predator–prey model with an SIRS disease in the predator, although the focus of the complex dynamics is on cases with saturating forces of infection. Siekmann et al. (2010) found bistability when adding a free-living virus stage to models of a predator–prey system with disease in the prey. Kooi et al. (2011) found period-doubling cascades into chaos, bistability and transcritical bifurcations of limit cycles. However, the existence of chaos in this model is not surprising, since the model is the same as the three-species Rosenzweig–MacArthur food chain model that was found to be chaotic in Hastings and Powell (1991).

In this paper, we explore two relatively simple eco-epidemiological models and demonstrate that a multitude of complex dynamics occurs. Such an array of complex dynamics has rarely been seen before. In Sect. 2, the models are introduced and explained, whereas Sect. 3 is a discussion on the steady states of these models and their stability. Together, these two sections give the background (the "basic" dynamics) for the main results in Sect. 4. These main results include bistability of limit cycles, turning points of limit cycles, a period-doubling cascade into chaos, tristability and a stable torus and its homoclinic destruction. All these results are a consequence of the disease since they do not occur in the disease-free predator–prey system.

2 The Models

We will introduce two similar models, one of which is the model in Hilker and Schmitz (2008) and uses frequency dependent transmission. The other model is the

diseased predator model in Bate and Hilker (2013), which is the analogue with density dependent transmission. We will start by describing their similarities before working on each model individually.

For both models, prey density X grows logistically to a carrying capacity K in the absence of predators. In the absence of prey, the predators die out exponentially. Predation is based on a Holling type II functional response and the predator's numerical response is proportional to total predation. Predators are infected by an SI disease, i.e. infection is for life and there is no immunity. Susceptible and infected predators are denoted by the densities S and I, respectively. All predators are born susceptible; there is no vertical transmission from infected mother to offspring. Infected predators suffer an additional disease-induced death rate, but otherwise behave in the same way as susceptible predators.

Starting with a prey–susceptible predator–infected predator model formulation, we will reformulate the models in terms of the total predator and prey populations and the prevalence of the disease in the predator population, i.e. the fraction of predators that are infected. This scaling is used to demonstrate the effect of the disease on the predator in the predator–prey system, something that is not immediately clear when the predator population is in two classes.

2.1 Density Dependent Transmission (DD Model)

Incorporating all these assumptions with a density dependent force of infection gives:

$$\frac{dX}{dT} = bX\left(1 - \frac{X}{K}\right) - \frac{aX(S+I)}{H+X}, \tag{1}$$

$$\frac{dS}{dT} = \frac{eaX(S+I)}{H+X} - dS - \sigma SI, \tag{2}$$

$$\frac{dI}{dT} = \sigma SI - (d+\alpha)I, \tag{3}$$

where b is the per capita growth rate of the prey when rare, K the carrying capacity of the prey, H the half-saturation population density, a the maximum predation rate per predator per prey, e the biomass conversion constant, d the natural per capita death rate of the predator, α the disease-induced per capita death rate of the predator and σ the transmissibility coefficient.

Setting $Y = S + I$ as the total predator density and $i = \frac{I}{Y}$ to be the prevalence, i.e. the proportion of infected predators, we get:

$$\frac{dX}{dT} = bX\left(1 - \frac{X}{K}\right) - \frac{aXY}{H+X}, \tag{4}$$

$$\frac{dY}{dT} = \frac{eaXY}{H+X} - dY - \alpha Yi, \tag{5}$$

$$\frac{di}{dT} = i\left((\sigma Y - \alpha)(1-i) - \frac{eaX}{H+X}\right). \tag{6}$$

To reduce the number of parameters, we can rescale using $X = NK$, $Y = eKP$ and $T = \frac{t}{ea}$ to get:

$$\frac{dN}{dt} = rN(1-N) - \frac{NP}{h+N}, \tag{7}$$

$$\frac{dP}{dt} = \frac{NP}{h+N} - mP - \mu Pi, \tag{8}$$

$$\frac{di}{dt} = i\left((\beta P - \mu)(1-i) - \frac{N}{h+N}\right), \tag{9}$$

where $r = \frac{b}{ea}$, $h = \frac{H}{K}$, $m = \frac{d}{ea}$, $\mu = \frac{\alpha}{ea}$ and $\beta = \frac{\sigma K}{a}$.

2.2 Frequency Dependent Transmission (FD Model)

Using the same argument, we arrive at the frequency dependent model, the same model as that in Hilker and Schmitz (2008). The parameters are the same as in the density dependent model except that the transmissibility carries a different unit and its dimensionless analogue is rescaled to $\beta = \frac{\sigma}{ea}$. This means that:

$$\frac{dX}{dT} = bX\left(1 - \frac{X}{K}\right) - \frac{aX(S+I)}{H+X}, \tag{10}$$

$$\frac{dS}{dT} = \frac{eaX(S+I)}{H+X} - dS - \sigma\frac{SI}{S+I}, \tag{11}$$

$$\frac{dI}{dT} = \sigma\frac{SI}{S+I} - (d+\alpha)I, \tag{12}$$

becomes

$$\frac{dN}{dt} = rN(1-N) - \frac{NP}{h+N}, \tag{13}$$

$$\frac{dP}{dt} = \frac{NP}{h+N} - mP - \mu Pi, \tag{14}$$

$$\frac{di}{dt} = i\left((\beta - \mu)(1-i) - \frac{N}{h+N}\right). \tag{15}$$

Notice that (13)–(15) are almost identical to (7)–(9), the difference being that (9) has a βP term whereas (15) has a β term.

3 Steady States and Stability

In this section, we will give a brief summary of the steady states and their stability. For more details, see the Appendix.

For both models, we have the extinction steady state $(0, 0, 0)$ and the prey-only disease-free steady state $(1, 0, 0)$. The former is always unstable, whereas the latter

is stable when the natural mortality rate of the predators is too high (i.e. $m > \frac{1}{h+1}$). Additionally, the FD model has a disease-induced predator extinction steady state $(1, 0, i^*)$, where $i^* = 1 - \frac{1}{(\beta-\mu)(1+h)}$. This occurs when the total mortality rate (natural plus disease-induced) of the predators is too high (i.e. $m + \mu i^* > \frac{1}{h+1}$). Notice that this can never happen if $m + \mu < \frac{1}{h+1}$.

There can be two other steady states; the disease-free predator–prey steady state $(N^*, P^*, 0)$ and the coexistent (predator–prey–disease) steady state (N^*, P^*, i^*). There is a transcritical bifurcation between these at $R_0^* = 1$ (the equilibrium-based basic reproductive number, Bate and Hilker 2013). For the FD model, the coexistent steady state is always unique when it exists. However, for the DD model, there can be up to two coexistent steady states. This opens up the possibility of saddle–node and backward bifurcations of the coexistent steady states.

Finding all the steady states does not give the full story. The underlying predator–prey system is the Rosenzweig–MacArthur model (1963), which is well known for having oscillatory dynamics caused by a Hopf bifurcation. Hence, by continuity, oscillations should occur in the predator–prey–disease system. Given the existence of stable oscillations, numerical results will be necessary. All bifurcation diagrams are plotted in MATLAB, mostly using data from the continuation software XPPAUT or multiple runs of "ode45" or "ode15s" in MATLAB. Equations in MATLAB are "log transformed" to prevent numerical errors dominating dynamics around zero. MATCONT is used for the two-parameter bifurcation diagram in Fig. 3(a).

4 Results

In this section, we will analyse and compare various complex dynamics that have been found in both models when there exist stable predator–prey oscillations in the absence of the disease (so parameters are chosen such that $m < \frac{1-h}{1+h}$). This analysis is largely done by varying the disease transmissibility (β) and the disease-induced death rate (μ). First, we will describe some general results that apply to either model. Then we will focus on various forms of bistability that can be found in these models. Furthermore, we will demonstrate that the DD model can exhibit tristability, a stable torus and its destruction via a homoclinic bifurcation; whereas the FD model can exhibit chaos via a period-doubling cascade. Lastly, we will describe various forms of regime shifts and hysteresis.

4.1 General Results

Figures 1(a)–(d) are bifurcation diagrams with respect to transmissibility (β) for the FD and DD models, respectively. When transmissibility is small, the disease can not spread fast enough to survive in the long run and thus only disease-free predator–prey oscillations are stable. As transmissibility increases, it will reach a threshold value corresponding to $\overline{R_0} = 1$, above which the disease will become endemic in the predator–prey oscillations, giving coexistent oscillations (Fig. 1(d)). Increasing transmissibility further results in the stabilisation of the coexistent oscillations via

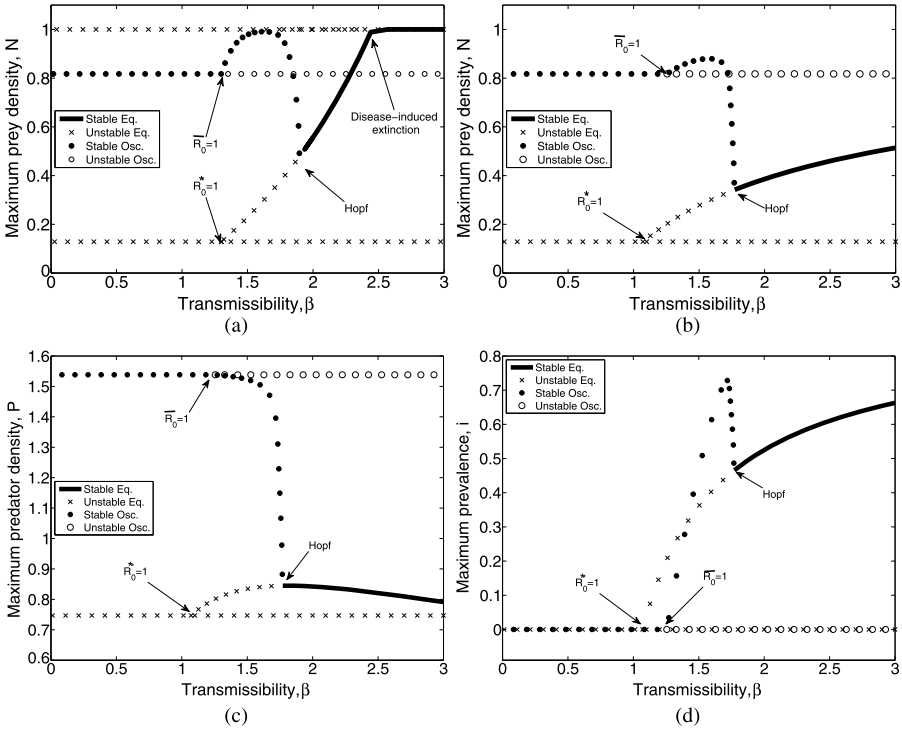

Fig. 1 Bifurcation diagrams of (**a**) the FD model and (**b**), (**c**), (**d**) the DD model, demonstrating the progression (with increasing transmissibility) from disease-free oscillations to endemic oscillations to an endemic equilibrium and, in (**a**) only, to disease-induced extinction of the predators. (**a**) and (**b**) show the (maximum) prey density (N) with respect to transmissibility (β), whereas (**c**) and (**d**) show maximum predator density and maximum prevalence, respectively. The trivial steady states have been omitted as well as the prey only steady state in (**b**). (**b**) is the same as Fig. 1 in Bate and Hilker (2013), whereas (**a**) is comparable to Fig. 2(a) in Hilker and Schmitz (2008) (but with different parameter values). Parameter values: (**a**) $\mu = 1$, $r = 1$, $h = 0.3$ and $m = 0.3$ (FD model); (**b**), (**c**), (**d**) $\mu = 0.5$, $r = 2$, $h = 0.3$, and $m = 0.3$ (DD model)

a Hopf bifurcation, leading to a stable coexistent equilibrium. The reason for stabilisation is that the total death rate of predators ($m + \mu i^*$) is now large enough to prevent predator–prey oscillations. However, this depends on a sufficiently large disease-induced death rate μ.

In addition to these common effects between the two models, there are aspects that only exist in one of the models.

For the FD model, a disease-induced extinction of the predators can occur when transmissibility (β) (and disease-induced death rate μ) are particularly large (Fig. 1(a)). This is not possible in the DD model since the disease can not survive when the density of predators becomes small, whereas the disease in the FD model can persist at any predator density, provided transmissibility is sufficiently large.

For the DD model (Fig. 1(b)), there is a difference between the transcritical bifurcation in the (stable) predator–prey oscillations ($\overline{R_0} = 1$) and the transcritical bifurcation in the (unstable) predator–prey equilibrium ($R_0^* = 1$). This means that the disease

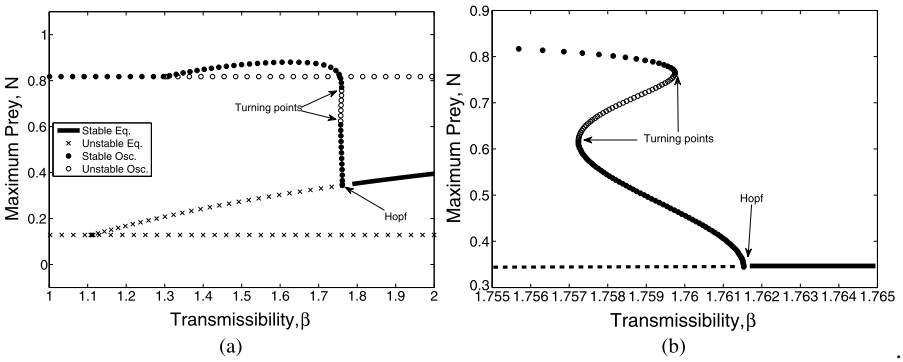

Fig. 2 Bistability between two limit cycles in the DD model. (**a**) demonstrates that bistability occurs for values of β between the two turning points of limit cycles, whereas (**b**) zooms in on the turning points of the limit cycles. There is also similar bistability in the FD model. In (**b**), the disease-free oscillations are not shown and stable/unstable equilibria have been drawn in for clarity, with the *dashed line* representing unstable equilibrium. $\mu = 0.53$. Other parameters are the same as Fig. 1(b)

has a different endemic threshold in predator–prey oscillations than at equilibrium (Fig. 1(d)). This difference in thresholds occurs because the time-averaged predator density for predator–prey oscillations is smaller than the predator density for the (unstable) predator–prey equilibrium in Rosenzweig–MacArthur predator–prey models. In the FD model, the thresholds at equilibrium and in oscillations are the same since the thresholds are independent of predator density, i.e. $R_0^* = \overline{R_0} = \frac{\beta}{m+\mu}$. The difference between the thresholds $R_0^* = 1$ and $\overline{R_0} = 1$ has been explored in more detail in Bate and Hilker (2013). As we will find out in the next subsection, this difference can lead to an interesting form of bistability between the endemic equilibrium and disease-free predator–prey oscillations in the DD model.

4.2 Various Forms of Bistability

In this subsection, we will demonstrate the birth of bistability via a cusp bifurcation of limit cycles and a generalised Hopf bifurcation in both the DD and FD models. We then discuss various forms of bistability, including bistability between endemic and disease-free states in the DD model.

Figure 2(a) is a bifurcation diagram with respect to transmissibility (β) for the DD model, like Fig. 1(b), but with a slightly increased disease-induced death rate ($\mu = 0.53$ instead of $\mu = 0.5$ in Fig. 1(b)). Both figures are quite similar with respect to the overall pattern from low to high transmissibility (β) of disease-free oscillations to coexistent oscillations to coexistent equilibria. There is, however, one major difference; namely, there are two turning points of limit cycles in the coexistent oscillations branch. Zooming in around the turning points makes this difference much clearer (Fig. 2(b)). Due to these two turning points of limit cycles, there are parameter regions with three coexistent limit cycles; the inner and outer limit cycles are stable (black circles in Fig. 2(b)), whereas the middle limit cycle (the one that joins the two turning points of limit cycles) is unstable (white circles in Fig. 2(b)). Thus there is bistability between two different limit cycles.

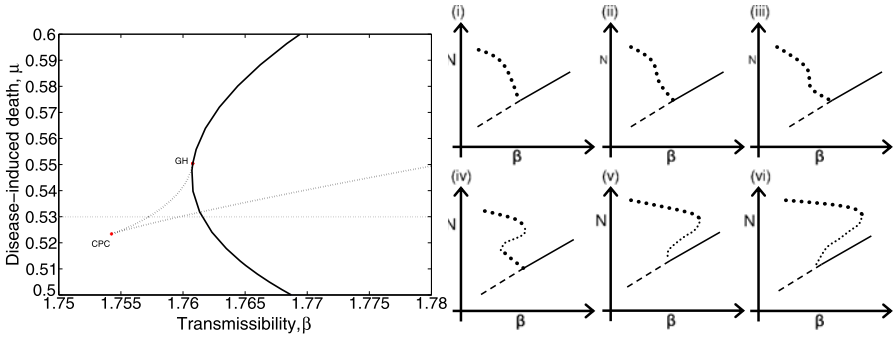

Fig. 3 The birth of bistability: (**a**) is a two-parameter bifurcation diagram with varying transmissibility (β) and disease-induced death rate (μ). This demonstrates that the bistability in Fig. 2 is the result of a cusp bifurcation of turning points of limit cycles between Fig. 1(b) and Fig. 2 (marked '*CPC*' for Cusp Point of Cycles). Further increases of μ lead to bistability between an equilibrium and a limit cycle (once beyond the generalised Hopf bifurcation, marked "*GH*"). For (**a**), the *thick dashed lines* represent the turning points of limit cycles, the *bold line* represents the Hopf bifurcation, and the *grey dashed horizontal line* highlights where Fig. 2 fits in. (**b**) is a sequence of sketched bifurcation diagrams with respect to transmissibility (β) for increasing disease-induced death rate (μ). For (**b**), *large black circles* stand for stable (endemic) oscillations, and *small black circles* stand for unstable (endemic) oscillations. Starting with a stable limit cycle (*i*) ($\mu = 0.5$, see Fig. 1(b)), the system progresses to the limit cycle beginning to "bow" (*ii*) ($\mu = 0.52$); to an inflection point in the limit cycle (cusp point) (*iii*) ($\mu \approx 0.5235$); to two stable limit cycles and one unstable limit cycle (*iv*) ($\mu = 0.53$, see Fig. 2); to a generalised Hopf bifurcation (*v*) ($\mu \approx 0.55$); to a subcritical Hopf bifurcation with one stable and one unstable endemic cycle (*vi*) ($\mu = 0.6$). A similar progression occurs in the FD model: $\mu = 1$ (see Fig. 1(a)) (*i*), $\mu = 2.4$ (*ii*), $\mu \approx 2.47$ (*iii*), $\mu = 3$ (*iv*), $\mu \approx 3.35$ (*v*) and $\mu = 3.5$ (*vi*). Other parameters. DD model: same as Fig. 1(b). FD model: same as Fig. 1(a)

Figure 3 demonstrates how two turning points of limit cycles can arise, as well as how this can lead to a subcritical Hopf bifurcation. We start the sequence in Fig. 3(b)(i) (bottom of Fig. 3(a)) with a solitary (coexistent) limit cycle just like in Fig. 1. Increasing μ results in the limit cycle branch being bowed in the middle much like a reverse "$\int$" (Fig. 3(b)(ii)). Instantaneously, this bowing results in an inflection point, also called a cusp point or bifurcation of the limit cycle (Fig. 3(b)(iii)). This is shown by the "CPC" in Fig. 3(a). Beyond this inflection point, there are two turning points (i.e. two saddle–nodes bifurcations) of limit cycles (Fig. 3(b)(iv)). In between these, there are three limit cycles; one stable limit cycle with small amplitude oscillations, one stable limit cycle with large amplitude oscillations and one unstable limit cycle that is between the other two. Thus, there is bistability between two different limit cycles, one with large amplitude and one with small amplitude.

Further increasing μ results in the two turning points spreading apart, and at some point the top/outer limit cycle goes beyond the Hopf bifurcation (when one of the dashed lines moves to the right of the bold Hopf line in Fig. 3(a)). From this point on, there is some parameter region where there is bistability between the large-amplitude limit cycle and the coexistent steady state. Increasing μ further moves the inner turning point closer to the Hopf bifurcation until they collide resulting in a generalised Hopf bifurcation (Fig. 3(b)(v)). This generalised Hopf bifurcation is marked "GH" in Fig. 3(a). Increasing μ beyond this, there is a subcritical Hopf bifurcation and only

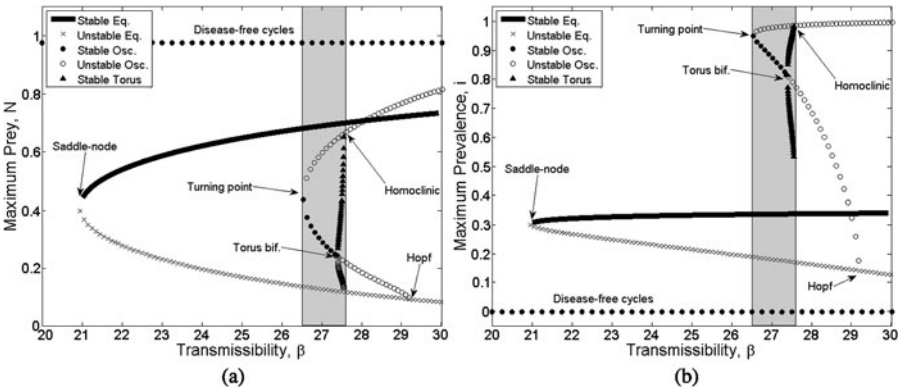

Fig. 4 Tristability and torus bifurcations in the DD model: Bifurcation diagrams of (**a**) maximum prey density (N) and (**b**) maximum prevalence, with respect to transmissibility (β) focused around the Hopf and saddle–node bifurcations. The *grey region* highlights a region of tristability between disease-free predator–prey oscillations, a coexistent equilibrium and coexistent limit cycle or torus. In this figure, both $R_0^* < 1$ and $\overline{R_0} < 1$, yet there are two endemic states in the grey region. Parameter values: $\mu = 2$, $r = 0.5$, $h = 0.1$ and $m = 0.2$. The disease-free predator–prey equilibrium is omitted; it is a *horizontal line* near the *horizontal-axis* ($N = 0.025$). The parameter region where the disease invades the predator–prey oscillation has been omitted

one turning point (Fig. 3(b)(vi)). In this case, there is bistability only between the outer coexistent limit cycle and the coexistent equilibrium.

This bifurcation sequence occurs in both the DD and FD models (see caption of Fig. 3). Consequently, both models can exhibit bistability between either two coexistent oscillations (one with large-amplitude and one with small-amplitude) or between a coexistent oscillation and a coexistent equilibrium. There is another form of bistability that, to the authors' knowledge, can only occur in the DD model: bistability between the coexistent equilibrium (or small-amplitude coexistent oscillations) and disease-free oscillations. This occurs when the Hopf bifurcation is to the left of the transcritical bifurcation of limit cycles at $\overline{R_0} = 1$ (Fig. 4 is an example of this kind of bistability). Bistability in the DD model between coexistent equilibria and either coexistent or disease-free oscillations model has also been found in Hurtado et al. (2013), although they dismiss such bistability occurring in the FD model.

4.3 Torus Bifurcations and Tristability

Figure 4 illustrates many phenomena not shown previously in this paper:

1. There is a saddle–node bifurcation of the coexistent equilibrium.
2. There is bistability between disease-free oscillations and coexistent equilibria. Normally, this bistability occurs when the Hopf bifurcation is to the left of the transcritical bifurcation of limit cycles. However, if the Hopf bifurcation is on the lower "saddle" branch of equilibria (like in Fig. 4) this bistability occurs when the saddle–node bifurcation is to the left of the transcritical bifurcation of limit cycles.
3. The saddle–node and Hopf bifurcations have switched positions (previously, the Hopf bifurcation was located on the upper "node" branch of equilibria, whereas

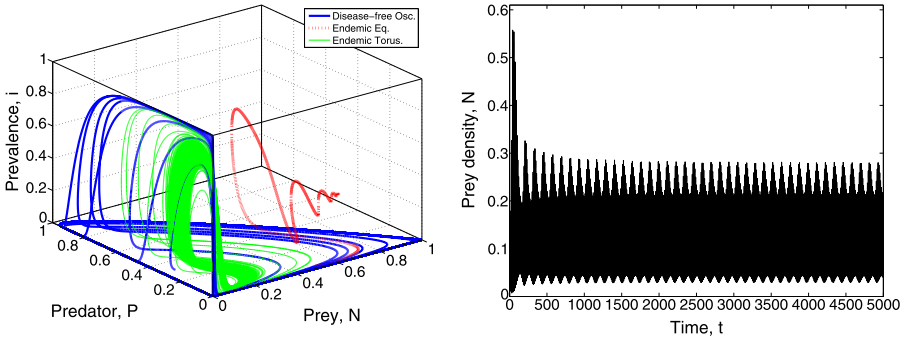

Fig. 5 (**a**) Phase portrait illustrating tristability in the DD model and (**b**) a time profile of the coexistent torus with respect to prey density (N). Initial conditions are (0.05, 0.3, 0.01) (disease-free oscillations), (0.5, 0.01, 0.01) (coexistent equilibrium) and (0.1, 0.2, 0.01) (coexistent torus). $\beta = 27.4$. Other parameters are the same as Fig. 4

in Fig. 4, the Hopf bifurcation is located on the lower "saddle" branch of equilibria). This means that a fold–Hopf bifurcation (sometimes called a zero–Hopf bifurcation) has occurred when the two bifurcations meet.

4. Along the unstable limit cycle arising from the Hopf bifurcation, a torus bifurcation occurs, which stabilises the limit cycle until a turning point of limit cycles is reached.
5. The stable torus created at the torus bifurcation is destroyed by a homoclinic bifurcation as the torus collides with the saddle limit cycle. Between the turning point of limit cycles and the homoclinic destruction of the torus, there is a region of tristability (the grey region of Fig. 4). Figure 5(a) demonstrates this tristability by showing that three different attractors can be obtained just by changing the initial condition, whereas Fig. 5(b) demonstrates that the toric attractor gives quasiperiodic dynamics.

The cause of the tristability seems to be the combination of (i) the Hopf bifurcation colliding with the saddle–node bifurcation, creating a fold–Hopf bifurcation, and (ii) a generalised Hopf bifurcation leading to the creation of a turning point of limit cycles near the Hopf bifurcation (like in Fig. 3) occurring soon after the fold–Hopf bifurcation. By varying the diseased-induced death rate, μ, and assuming all other parameters are the same as Fig. 4, tristability occurs for values of μ beyond the fold–Hopf bifurcation ($\mu \approx 0.95$) and the generalised Hopf bifurcation ($\mu \approx 0.97$), i.e. tristability occurs for $\mu \gtrsim 0.97$.

The torus that appears at the (supercritical) torus bifurcation grows until it collides with another invariant set. In Fig. 4 ($\mu = 2$), the torus breaks down as it seems to collide with the saddle limit cycle to form a homoclinic orbit. (This is clearer in Fig. 4(b) since in Fig. 4(a), the torus looks like it is close to the unstable equilibrium at the homoclinic bifurcation, which is not the case). Figures 6(a) and (b) are Poincaré sections before and after this homoclinic bifurcation, respectively, showing the homoclinic destruction of the torus. Figure 6(a) shows a closed loop in the Poincaré section, consistent with quasiperiodic dynamics on a stable torus, whereas Fig. 6(b)

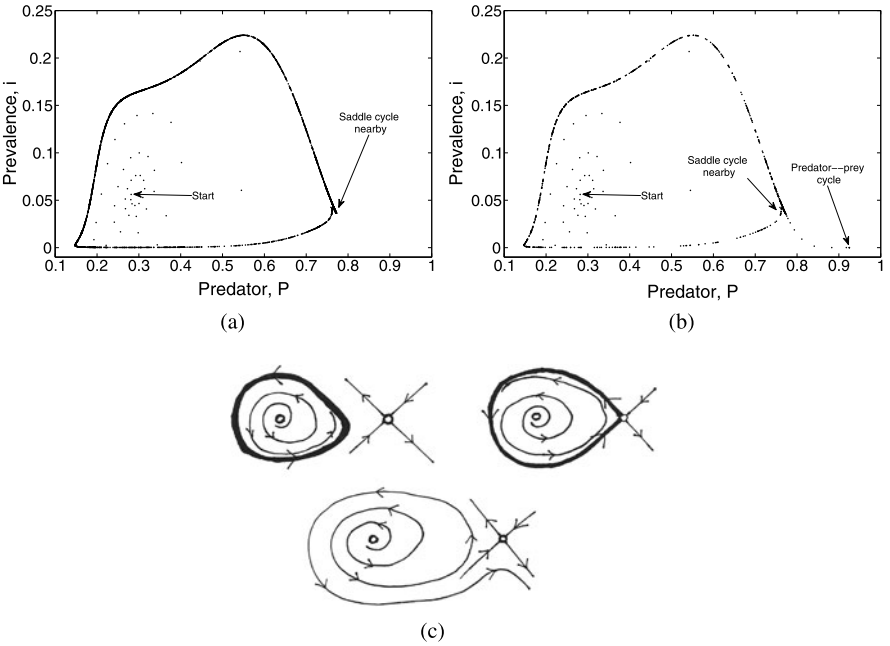

Fig. 6 Poincaré sections demonstrating the destruction of the torus in Fig. 4 in the DD model: (**a**) just before the homoclinic destruction of the torus ($\beta = 27.54513$), (**b**) just after the homoclinic destruction of the torus ($\beta = 27.54514$). Notice the *curve in the Poincaré section* (torus) is sparser in (**b**) since the system follows the cycle several times in a transient phase before going to the predator–prey oscillations. The Poincaré section is of trajectories hitting the $N = 0.12$ plane from above. (**c**) is a sketch of the creation and destruction of the homoclinic orbit in the Poincaré section, where the *white circles* represent unstable (or saddle) limit cycles, *thick lines* represent the stable torus, and the *thin lines with arrows* represent either the trajectories, or the stable/unstable manifolds of the saddle-limit cycle. Other parameters are the same as Fig. 4

shows a loop in the Poincaré section that is broken after many iterations, consistent with a long quasiperiodic transient. Figure 6(c) is a sketch of the mechanism behind the homoclinic destruction of the torus. The saddle limit cycle (seen as a saddle point in the Poincaré section) and stable torus (seen as a stable limit cycle in the Poincaré section) approach each other (top left of Fig. 6(c)). Instantaneously, the stable torus and saddle limit cycle collide to form a homoclinic orbit in the Poincaré section (top right of Fig. 6(c)). Beyond this, although there are quasiperiodic transients, the stable torus no longer exists, leaving just the saddle limit cycle and unstable limit cycle (bottom middle of Fig. 6(c)). In the case of Fig. 4, after the homoclinic destruction of the torus, trajectories near the original torus seem to eventually converge to the disease-free predator–prey oscillations, after some quasiperiodic transient.

The existence of a stable torus should not be too much of a surprise. In fact, Kuznetsov (1995, p. 300) states that fold–Hopf bifurcations, the interaction between fold (i.e. saddle–node) and Hopf bifurcations, can lead to tori. In the FD model, however, torus bifurcations and tristability have not been found. The reason is that there is no "fold" in the FD model. Likewise, there is no saddle–node bifurcation to provide a second equilibrium branch which may lead to another set of stable dynamics. Con-

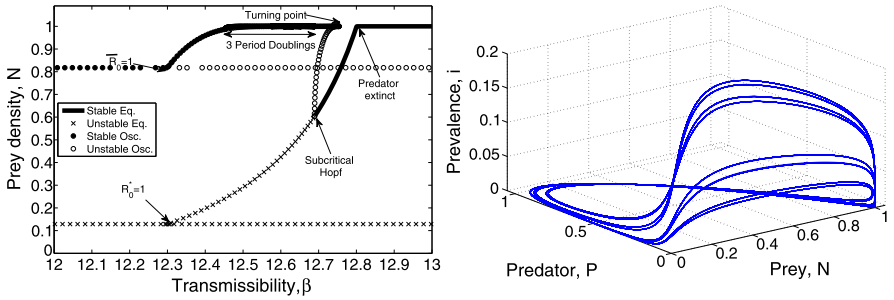

(a) (b)

Fig. 7 Period-doubling in the FD model: (**a**) Bifurcation diagram with respect to β where $\mu = 12$. Three period-doubling bifurcations have occurred, although this is not clear as all branches are very close to each other. To confirm the existence of three period doubling bifurcations, (**b**) shows a phase portrait of the resulting 8-cycle at $\beta = 12.62$ $(= \mu + 0.62)$. Other parameters are the same as Fig. 1(a)

sequently, the frequency dependent model probably does not have either tristability or invariant tori, although we can not exclude these phenomena.

It is worth noting that in this scenario, "living on the torus" can be a reasonably good scenario for the disease, predator and prey. For $\beta = 27.4$, the minimum values are $N \approx \exp(-3.5)$, $P \approx \exp(-4)$ and $i \approx \exp(-11)$, whereas near the homoclinic orbit at $\beta = 27.54513$ (Fig. 6(a)) the lows are $N \approx \exp(-5)$, $P \approx \exp(-6)$ and $i \approx \exp(-25)$. For example, if β increases from a region with a stable torus to a region where it has broken down, trajectories near the previously stable torus will now eventually approach (after some quasiperiodic transient) the disease free predator–prey oscillations. These oscillations have much more severe lows for both predator and prey (approximately $\exp(-19)$ and $\exp(-43)$, respectively) which in reality could lead to stochastic extinction of the predator and/or prey.

At $\mu = 1$ (with other parameters the same as Fig. 4), there is a similar torus/limit cycle tristability (since $\mu \gtrsim 0.97$). However, the parameter region is very small, which also makes it more difficult to numerically investigate how the torus disappears. In this case, the lows of each variable are not as severe as the case of $\mu = 2$ (Fig. 4). The authors suspect that this breakdown is either the result of the same homoclinic orbit at the saddle limit cycle or the "hole" of the torus shrinks to nothing, colliding with the unstable (saddle point) steady state it surrounds. Following the breakdown of this torus for $\mu = 1$, after some quasiperiodic transient, the system seems to settle down at the endemic equilibrium, which is different to the $\mu = 2$ (Fig. 4) case where the disease-free oscillations are approached.

4.4 Period-Doubling and Chaos

In the FD model, increasing the disease-induced death rate (μ), period-doubling bifurcations begin to arise. By the time $\mu = 12$, three period-doubling bifurcations have occurred (Fig. 7(a)), resulting in the existence of an "8-cycle" (Fig. 7(b)). Figure 8 demonstrates that these period-doubling bifurcations form part of a period-doubling cascade, which results in chaotic dynamics soon after $\mu = 12$.

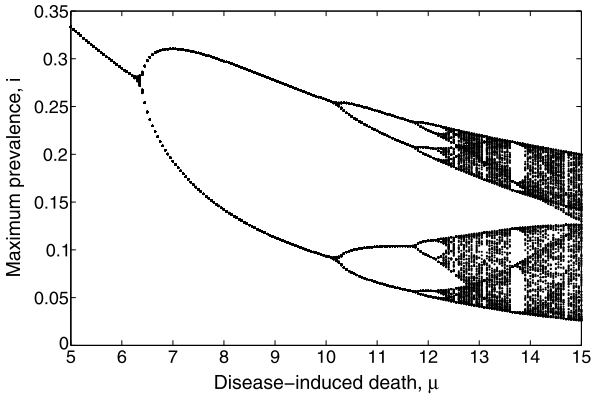

Fig. 8 Period-doubling cascade into chaos in the FD model. Bifurcation diagram of (local) maximum prevalence with respect to μ, where β varies with μ along the line $\beta = \mu + 0.62$. Other parameters are the same as Figs. 1(a) and 7. The initial condition $(N, P, i) = (1, 0.1, 0.01)$ was used

We also have a region of bistability in Fig. 7(a), between coexistent limit cycles (including 2-cycles) and coexistent equilibria. This leads to the possibility of bistability between coexistent chaos and coexistent equilibria/small-amplitude limit cycles.

In the DD model, period-doubling bifurcations have not been found. However, we suspect that period-doubling bifurcations and the cascading into chaos phenomenon might exist in the DD model. Additionally, since bistability seems to be at least as common in the DD model, compared with the FD model, bistability between coexistent chaos and coexistent equilibria/small-amplitude limit cycles might also exist in the DD model.

4.5 Regime Shifts and Hystereses

There is one distinct phenomenon common to Figs. 2, 3, 4, 7; the possibility of regime shifts and hystereses. Regime shifts are large, abrupt, persistent changes in the structure and function of a system (Biggs et al. 2009). Here, we will restrict the definition of regime shifts to that of "critical transitions" from Scheffer (2009); the drastic change toward another state caused by minor perturbations and/or a gradual change in the system (i.e. parameters), This definition ignores drastic changes caused by large and sudden changes to the system. Using this definition, a regime shift occurs when there is a discontinuity (jump) in stable attractors when varying a particular parameter. Here, there are many different regime shifts because of the existence of saddle–node bifurcations, turning points of limit cycles, bistability, tristability and the homoclinic destruction of a stable torus. We will separate regime shifts into two different classes; (globally) reversible and (globally) irreversible.

A (globally) reversible regime shift is a regime shift such that there is a (possibly complex) sequence of small alterations in the bifurcation parameter that will lead back to the starting point, via a hysteresis loop. Notice that we mention globally, since we are describing recovering to the original state via some potentially long and complicated path and not by a small, local change. An example of a reversible regime is in Fig. 7; starting just to the left of the turning point of the coexistent oscillations, slowly increasing transmissibility beyond the turning point will mean that the system will eventually approach the coexistent equilibrium after some oscillatory transient. Now that we "sit" on the endemic equilibrium, reducing transmissibility slowly will

not deviate from the equilibrium until the Hopf bifurcation is passed, far below the original transmissibility. Below the Hopf bifurcation, the system will slowly approach the endemic oscillations (possibly a 2-cycle). Once there, slowly increasing the transmissibility will move the system toward the original state near the turning point on the endemic oscillations.

A (globally) irreversible regime shift is a regime shift where there is no such sequence of small alterations to get back to the starting point, i.e. there is no hysteresis loop. This means that once the system has moved away from the starting point, it can never return without a dramatically large perturbation away from another stable state. For example, in Fig. 4, there seems to be no plausible way of approaching the endemic limit cycle/torus via either stable oscillations or equilibria. This means when starting on the stable coexistent limit cycle/torus, slowly decreasing transmissibility below the turning point of coexistent oscillation or increasing transmissibility beyond the homoclinic destruction of the torus would lead to the end of coexistent limit cycle/torus forever.

5 Discussion

In this paper, we explored two relatively simple eco-epidemiological models and found an unusually large variety of complex dynamics. The variety of complex dynamics found in these models, which is summarised in Table 1, is much broader than in previous studies in eco-epidemiology and most studies in ecology and epidemiology.

We found that the Hopf bifurcation between the coexistent steady state and the coexistent periodic orbit can become subcritical, via a cusp bifurcation of limit cycles. Consequently, bistability between coexistent oscillations and coexistent equilibria or between two different coexistent oscillations can occur in both the DD and FD models. Combining this with the fact that there is a difference between R_0^* and $\overline{R_0}$ in the DD model (see Bate and Hilker 2013, for more details) there are also scenarios where there is bistability between a coexistent equilibrium and disease-free predator–prey oscillations. In these scenarios, it is the initial condition that determines whether the disease can become endemic to a stable equilibrium or not. In particular, if the saddle–node bifurcation is biologically realistic, there are scenarios where the disease is endemic (at equilibrium, oscillation or torus, Fig. 4) despite both R_0^* and $\overline{R_0}$ being less than one. This is reminiscent of a backward bifurcation, a phenomenon found in a few epidemiological models like some in van den Driessche and Watmough (2002).

In the previous paragraph, we concluded that that the disease can persist despite both R_0^* and $\overline{R_0}$ being less than one. However, we can say more; Fig. 4 demonstrates that there can be two stable coexistent states despite both R_0^* and $\overline{R_0}$ being less than one. This goes beyond the usual backward bifurcation since Fig. 4 demonstrates that the disease can persist in two stable states, one stable state is an equilibrium whereas the other is (quasi-)oscillatory, despite both R_0^* and $\overline{R_0}$ being less than one.

We demonstrated that period-doubling exists in the FD model. In fact, we have shown that period-doubling bifurcations can cascade into chaos. We have not found period-doubling in the DD model, however, the authors believe that period-doubling bifurcations (and the cascade into chaos) might occur.

Table 1 Summary of complex dynamics found in the DD and FD models

	FD model	DD model
Disease stabilisation	✓ (Hilker and Schmitz 2008)	✓ (Figs. 1(b)–(d))
Different endemic thresholds	✗, $R_0^* = \overline{R_0}$ (Bate and Hilker 2013)	✓, $R_0^* > \overline{R_0}$ (Bate and Hilker 2013)
S–N bifurcation of Eq	✗ (the Appendix)	✓ (Fig. 4)
S–N bifurcation of LC (turning points)	✓ (Figs. 2, 3)	✓ (Figs. 2, 3)
Subcritical Hopf	✓ (Figs. 3, 7(a))	✓ (Fig. 3)
Cusp bifurcation of LC	✓ (Fig. 3)	✓ (Fig. 3)
Bistability …	✓	✓
… between Co LC and Co Eq	✓ (Figs. 3, 7(a))	✓ (Fig. 3)
… between 2 Co LC	✓ (Figs. 2, 3)	✓ (Figs. 2, 3)
… between DF LC and Co Eq/LC	✗	✓ (Fig. 4)
… between Co Chaos and Co Eq/LC	✓? (Fig. 7)	✓?
Torus bifurcation	✗?	✓ (Fig. 4)
Homoclinic bifurcation	✗?	✓, destruction of torus (Figs. 4, 6)
Tristability	✗?	✓, between DF LC, Co Eq and Co LC/Torus (Figs. 4, 5)
Period doubling bifurcation	✓, cascades into chaos, (Figs. 7, 8)	✓?
Regime Shifts and hysteresis	✓, reversible found only	✓, reversible and irreversible

"✓" means found, "✗" means can not occur in this model, "✓?" means that not found in this paper but we suspect can occur in this model and "✗?" means that we do not believe this can occur but have not completely discounted it. "Co": Coexistent, "DF": Disease-free, "Eq": Equilibria, "LC": Limit cycles, "S–N": Saddle–Node

One result in this paper is the existence of hystereses and regime shifts. With all the bistability, tristability and homoclinic orbits, there are many examples of regime shifts. Most of these regime shifts can be reversed via some long and complex sequence of small changes in parameter value. It is worth noting that such sequences may be impractical, not feasible, or downright impossible in reality. However, some regime shifts can not be reversed. In particular, we found that the stable coexistent torus/oscillations in Figs. 4, 5, 6 are not recoverable when lost without large perturbations.

One aspect that is novel in this paper is the scenario of tristability. Tristability seems particularly rare in ecological and epidemiological models. The authors are not aware of any previous examples of tristability in eco-epidemiological papers, with only a few works finding bistability (Siekmann et al. 2010; Kooi et al. 2011; Sieber and Hilker 2011). In fact, the most examples the authors have found of tristability in ecology or epidemiology typically involve one or more Allee effects. For example, Hilker et al. (2009) found tristability when adding disease to a population with an Allee effect, whereas González-Olivares and Rojas-Palma (2011) found tristability when combining a predator–prey interaction with a Holling type III functional response and an Allee effect in the prey. Likewise, Berezovskaya et al. (2010)

found tristability when considering a predator–prey interaction with linear functional response, prey refuge and an Allee effect in the prey. Tristability in these models is not particularly surprising; Allee effects usually imply bistability, so tristability only requires the creation of one unexpected stable equilibrium or limit cycle. An example of tristability that does not involve Allee effects is found in Beardmore and White (2001); here there is an infectious disease in a population with complex social group structure. All these papers have one aspect in common, the tristability is between several equilibria (Beardmore and White 2001; Hilker et al. 2009) or two equilibria and an oscillation (Hilker et al. 2009; González-Olivares and Rojas-Palma 2011; Berezovskaya et al. 2010), with one or more of the equilibria being (semi-)trivial. In this paper, the tristability is between a disease-free (semi-trivial) oscillation and two coexistent states, one equilibrium and one (quasi-)oscillatory. However, both coexistent states, as previously mentioned, are not expected to exist from the usual "R_0 argument" as both $R_0^* < 1$ and $\overline{R_0} < 1$. On top of this, the coexistent torus/limit cycle in Fig. 6 can not be found by the usual steady state and stability analysis.

We can confirm that a disease with density dependent transmission can have the same stabilising affect as the disease with frequency dependent transmission has on a predator found in Hilker and Schmitz (2008), taking predator–prey oscillations to endemic equilibrium. The reason why this occurs is that the disease increases total host mortality (from mP to $(m + \mu i)P$), which will dampen the boom and bust of Rosenzweig–MacArthur predator–prey dynamics. Also, we have demonstrated that disease in the predators can greatly influence not only predator (host) density, but also interacting species like the prey.

The models used in this paper are relatively simple for eco-epidemiological models as the disease only increases host mortality. This means infection does not change how effective the predator is at searching, handling and eating prey as well as reproduction. This point is particularly clear in the predator–prey-prevalence equations (7)–(9) and (13)–(15), where the disease has no direct influence on total prey density and only influences the predator population via additional mortality. Likewise, the disease is only an SI disease, with no recovery, latency or immunity. Also, the models use the standard frequency dependent and density dependent forces of infection.

These two forces of infection are the two default choices when modelling disease transmission, largely because they are relatively simple and can be mechanistically derived using assumptions based on contact rates. However, in wildlife diseases, there have been mixed results to whether these forces of infections are realistic (McCallum et al. 2001; Ferrari et al. 2011). Despite this, they are still seen as the benchmarks of which all other forces of infection are compared (Begon et al. 2002).

The summary of results in Table 1 shows that density dependent and frequency dependent transmission can yield distinctly different dynamics. Note that tristability and different endemic thresholds between limit cycles and equilibrium are not possible with frequency dependent transmission. On top of this, there are relatively small regions of coexistence between predator and disease in the frequency dependent transmission if the disease-induced mortality (μ) is large. If more complex, non-linear forces of infection were used, one would expect some of the complex dynamics found in these models (especially the density dependent model, since many

non-linear forces of infection like those based on power laws or saturating contact rates can be simplified to a density dependent force of infection via parameter or limit assumptions) as well as other complex phenomena. In particular, the endemic thresholds R_0^* and $\overline{R_0}$ would be different for most forces of infection, with frequency dependent transmission being the main exception. This means that, unlike frequency dependent transmission, most forces of infection could have bistability between endemic and disease-free states. However, both models have bistability and both are suspected to have chaos following a period-doubling cascade, which suggests that such phenomena also exist for a wide range of forces of infection.

There is a caveat to some of these results in this paper, one that is common with many models that exhibit chaos and complex dynamics; dangerously small population sizes (Berryman and Millstein 1989; Thomas et al. 1980). Some of the interesting dynamics occur in scenarios of major boom and bust, cases that are likely to cause stochastic extinctions (this problem depends on the predator/prey rescaling; in particular, it depends on the carrying capacity of the prey in the original model, K). In particular, looking at the phase space plots illustrating tristability in Fig. 5, we can see that the predator–prey oscillations (and to a lesser extent the coexistent torus) get very close to the origin. Although various simulations were investigated, the search was not exhaustive and there may be parameter values that do not result in dramatic boom and bust, but still contain similar complex dynamics. For example, the torus at $\mu = 1$ (other parameters are the same as in Fig. 4) suffers less from the dangerously low populations than the example in Figs. 4, 5, 6 where $\mu = 2$. In particular, we only investigated scenarios where disease-free predator–prey oscillations exist. There could be scenarios where complex dynamics like oscillatory dynamics, bi/tristability and chaos occur when, in the absence of the disease, only stable equilibria exist; but we stress that this has not been investigated in this paper.

The existence of a torus bifurcation (sometimes called a Neimark–Sacker bifurcation) poses many unanswered questions. We have demonstrated one case where the torus seems to be broken by a homoclinic orbit of a saddle–cycle. However, there are many other ways how a torus can bifurcate or disappear. For example, the torus could experience period doubling bifurcations into chaos or there could be phase locking into a periodic orbit. The analysis in this paper is restricted to just one set of parameter values, largely because of the interesting case of tristability. This means there is much more to explore in relation to the stable torus than is found this paper.

The results in the FD model are directly comparable with Hilker and Schmitz (2008). Figure 1 uses parameter values not too dissimilar to those in Hilker and Schmitz (2008). As we make the disease dynamics "faster" (i.e. higher disease-induced death rate μ with higher transmissibility β), the system becomes more complex as bistability and period doubling cascades arise. However, increasing μ gives smaller ranges of β where coexistence can occur (complex or not). This makes it less likely for coexistence to occur for high μ, a point that can be seen in Hilker and Schmitz (2008, Fig. 4). In the DD model, we suspect a similar pattern for fast disease dynamics. However, there is no upper limit in transmissibility (β) for endemic coexistence since there is no disease-induced extinction of the predator in the DD model.

In the absence of the disease, the predator–prey interaction can only lead to two types of stable dynamics; stable equilibria and stable oscillations. This means that the

bistability, tristability, period-doubling into chaos, stable tori and homoclinic orbits (and much more, see Table 1) exist because of the interaction with the disease in the predator. The regimes of multistability imply that the eco-epidemic system may be extremely sensitive to perturbations (e.g. due to stochastic events, control actions like culling or gradual trends in environmental conditions). This can trigger a number of regime shifts, some of which we have identified to be irreversible. The regime shifts may also be accompanied by long-lasting transients of former attractors.

In summary, we can conclude that diseases can greatly influence the dynamics of the host population and other species interacting with the host. In other words, eco-epidemiology can give profoundly different results than just the background ecology. Similarly, predation can make disease dynamics more complicated.

Acknowledgements The authors would like to thank Faina Berezovsky and an anonymous reviewer for their constructive comments.

Appendix: Steady States of FD and DD Models

There are two key differences between the DD and FD model. One is the existence of a disease-induced extinction of the predator in the FD model. The other is that there can be only one coexistent steady state in the FD model as the corresponding value of i^* is known; whereas in the DD model, there can be one or two coexistent steady states.

A.1 Trivial/Semi-trivial Steady States

- Both models: $(0, 0, 0)$ which always exists and is always unstable.
- Both models: $(1, 0, 0)$ which always exists and is stable if $m > \frac{1}{1+h}$, unstable otherwise.
- Both models: $(N^*, P^*, 0)$, where $N^* = \frac{hm}{1-m}$ and $P^* = r(h + N^*)(1 - N^*)$. This exists when $m < \frac{1}{1+h}$ (< 1). It is stable if $N^* > \frac{1-h}{2}$ (equivalently $m > \frac{1-h}{1+h}$ (Hopf bifurcation)) and $R_0^* < 1$, where R_0^* equals $\frac{\beta P^*}{m+\mu}$ (DD model) and $\frac{\beta}{m+\mu}$ (FD model).
- FD model only: $(1, 0, i^*)$ where $i^* = 1 - \frac{1}{(\beta-\mu)(1+h)}$. This exists when $\beta - \mu > \frac{1}{1+h}$ and is stable if $m + \mu i^* > \frac{1}{1+h}$, unstable otherwise.
- (FD model only: $(0, 0, 1)$. This is always unstable.)
- (FD model only: $(0, 0, i^*)$. i^* is unspecified. This only exists when $\beta = \mu$, which is not generally true. This is always unstable.)

A.2 Coexistent Steady State(s)

A.2.1 DD Model

The coexistent equilibria for the DD model are of the form (N^*, P^*, i^*), where $N^* = \frac{h(m+\mu i^*)}{1-(m+\mu i^*)}$, $P^* = r(h + N^*)(1 - N^*)$ and $i^* = 1 - \frac{N^*}{h+N^*}\frac{1}{\beta P^*-\mu} = 1 - \frac{m+\mu i^*}{\beta P^*-\mu} =$

$\frac{\mu(1-i^*)-m+\beta P^*}{\beta P^*-\mu}$. This exists when $i^* < \frac{1-m}{\mu}$ ($N^* > 0$), $i^* < \frac{1}{\mu(h+1)} - \frac{m}{\mu}$ ($N^* < 1$, i.e. $P^* > 0$), $P^* > \frac{\mu}{\beta}$ (for $i^* < 1$) and $P^* > \frac{\mu+m}{\beta}$ (for $i^* > 0$).

The strongest of these conditions are $i^* < \frac{1}{\mu(h+1)} - \frac{m}{\mu}$ and $P^* > \frac{\mu+m}{\beta}$, which are the conditions that $R_i^p > 1$ (the predators' reproductive number given an infection is present) and $R_0^* > 1$, (the diseases' reproductive number).

It is not clear whether (N^*, P^*, i^*) has only one solution. Consequently, this must be solved. For tidiness, let $D = m + \mu i^*$. Starting with $\frac{D-m}{\mu}$ $(= i^*)$, we get:

$$\frac{D-m}{\mu} = 1 - \frac{D}{\beta P - \mu} \tag{16}$$

$$= 1 - \frac{D}{\beta r(h+N)(1-N) - \mu} \tag{17}$$

$$= 1 - \frac{D}{\beta r(h + \frac{hD}{1-D})(1 - \frac{hD}{1-D}) - \mu} \tag{18}$$

$$= 1 - \frac{D(1-D)^2}{\beta r h(1-D-hD) - \mu(1-D)^2}. \tag{19}$$

After some further rearrangement, we get:

$$0 = \left(\frac{D-m}{\mu} - 1\right)\beta r h(1-D-hD) + (m+\mu)(1-D)^2. \tag{20}$$

This is clearly quadratic with respect to D, and thus i^*. D can only be biologically realistic if $D \in (m, m+\mu)$ (i.e. $i^* \in (0, 1)$). This means there are at most two feasible coexistent solutions.

The stability is not fully investigated. However, when these steady states exist, no other steady state is stable. Also, when there are two viable coexistent steady states, they will be connected to a nearby saddle–node bifurcation, so only one steady state should be stable. Given this, we expect would that either one of the coexistent equilibria is stable or there is some stable periodic solution.

A.2.2 FD Model

The coexistent steady state for the FD model is (N^*, P^*, i^*) where $N^* = \frac{h(m+\mu i^*)}{1-(m+\mu i^*)}$, $P^* = r(h+N^*)(1-N^*)$ and $i^* = 1 - \frac{\mu+m}{\beta}$. This exists when $\beta > \mu + m$ ($i^* > 0$), $i^* < \frac{1-m}{\mu}$ ($N^* > 0$), $i^* < \frac{1}{\mu(h+1)} - \frac{m}{\mu}$ ($N^* < 1$, i.e. $P^* > 0$). Like the DD model, the two strongest conditions are $i^* < \frac{1}{\mu(h+1)} - \frac{m}{\mu}$ and $\beta > \mu + m$. In this case, there is only one coexistent steady state if it exists.

The stability is not fully investigated. However, when this steady state exists, no other steady state is stable. Given this, we would expect that either one of the coexistent equilibria is stable or there is some stable periodic solution.

References

Bate, A. M., & Hilker, F. M. (2013). Predator–prey oscillations can shift when diseases become endemic. *J. Theor. Biol.*, *316*, 1–8.

Beardmore, I., & White, K. A. J. (2001). Spreading disease through social groupings in competition. *J. Theor. Biol.*, *212*, 253–269.

Begon, M., Bennett, M., Bowers, R. G., French, S. M., Hazel, N. P., & Turner, J. (2002). A classification of transmission terns in host-microparasite models: numbers, densities and areas. *Epidemiol. Infect.*, *129*, 147–153.

Berezovskaya, F. S., Song, B., & Castillo-Chavez, C. (2010). Role of prey dispersal and refuges on predator–prey dynamics. *SIAM J. Appl. Math.*, *70*, 1821–1839.

Berryman, A. A., & Millstein, J. A. (1989). Are ecological systems chaotic—and if not, why not? *Trends Ecol. Evol.*, *4*, 26–28.

Biggs, R., Carpenter, S. R., & Brock, W. A. (2009). Turning back from the brink: detecting an impending regime shift in time to avert it. *Proc. Natl. Acad. Sci. USA*, *106*, 826–831.

Chattopadhyay, J., & Bairagi, N. (2001). Pelicans at risk in Salton Sea—an eco-epidemiological model. *Ecol. Model.*, *136*, 103–112.

Ferrari, M. J., Perkins, S. E., Pomeroy, L. W., & Bjørnstad, O. N. (2011). Pathogens, social networks, and the paradox of transmission scaling. *Interdiscip. Perspect. Infect. Dis.*, *2011*, 267049.

Gilpin, M. E. (1979). Spiral chaos in a predator–prey model. *Am. Nat.*, *113*, 306–308.

González-Olivares, E., & Rojas-Palma, A. (2011). Multiple limit cycles in a Gause type predator–prey model with Holling type III functional response and Allee effect on prey. *Bull. Math. Biol.*, *73*, 1378–1397.

Hastings, A., & Powell, T. (1991). Chaos in a three-species food chain. *Ecology*, *72*, 896–903.

Hilker, F. M., & Malchow, H. (2006). Strange periodic attractors in prey–predator system with infected prey. *Math. Popul. Stud.*, *13*, 119–134.

Hilker, F. M., & Schmitz, K. (2008). Disease-induced stabilization of predator–prey oscillations. *J. Theor. Biol.*, *225*, 299–306.

Hilker, F. M., Langlais, M., & Malchow, H. (2009). The Allee effect and infectious diseases: extinction, multistability, and the (dis-)appearance of oscillations. *Am. Nat.*, *173*, 72–88.

Hurtado, P. J., Hall, S. R., & Ellner, S. P. (2013). Infectious disease in consumer populations: dynamic consequences of resource-mediated transmission and infectiousness, manuscript in review.

Kooi, B. W., van Voorn, G. A. K., & Das, K. p. (2011). Stabilization and complex dynamics in a predator–prey model with predator suffering from an infectious disease. *Ecol. Complex.*, *8*, 113–122.

Kuznetsov, Y. A. (1995). *Elements of applied bifurcation theory*. New York: Springer.

May, R. (1974). Biological populations with nonoverlapping generations: stable points, stable cycles, and chaos. *Science*, *186*, 645–647.

McCallum, H., Barlow, N., & Hone, J. (2001). How should pathogen transmission be modelled? *Trends Ecol. Evol.*, *16*, 295–300.

Rosenzweig, M. L., & MacArthur, R. H. (1963). Graphical representation and stability conditions of predator–prey interactions. *Am. Nat.*, *97*, 209–223.

Scheffer, M. (2009). *Critical transitions in nature and society*. Princeton: Princeton University Press.

Seydel, R. (1988). *From equilibrium to chaos—practical bifurcation and stability analysis*. New York: Elsevier.

Sieber, M., & Hilker, F. M. (2011). Prey, predators, parasites: intraguild predation or simpler community modules in disguise? *J. Anim. Ecol.*, *80*, 414–421.

Siekmann, I., Malchow, H., & Venturino, E. (2010). On competition of predators and prey infection. *Ecol. Complex.*, *7*, 446–457.

Stiefs, D., Venturino, E., & Feudel, U. (2009). Evidence of chaos in eco-epidemic model. *Math. Biosci. Eng.*, *6*, 855–871.

Thomas, W. R., Pomerantz, M. J., & Gilpin, M. E. (1980). Chaos, asymmetric growth and group selection for dynamical stability. *Ecology*, *61*, 1312–1320.

Upadhyay, R. K., Bairagi, N., Kundu, K., & Chattopadhyay, J. (2008). Chaos in eco-epidemiological problem of the Salton Sea and its possible control. *Appl. Math. Comput.*, *196*, 392–401.

van den Driessche, P., & Watmough, J. (2002). Reproductive numbers and sub-threshold endemic equilibria for compartmental models of disease transmission. *Math. Biosci.*, *180*, 29–48.